

International Journal of Sustainable Development and Planning

Vol. 20, No. 9, September, 2025, pp. 3973-3982

Journal homepage: http://iieta.org/journals/ijsdp

Economic and Technical Management in Environmental Impact Assessment of Floating Solar Power



Anh Lan Nguyen 10, Dat Hoang Vo 20, Anh Tu Le 30, Tuyen Ngoc Nguyen 40, Luu Dang Ngo 5*00

- ¹ Faculty of Business Administration, Industrial University of Ho Chi Minh City, Ho Chi Minh 700000, Vietnam
- ² Vinh Son Song Hinh Hydropower Joint Stock Company, Ho Chi Minh 700000, Vietnam
- ³ Faculty of Finance and Banking, Nghe An University, Ho Chi Minh 700000, Vietnam
- ⁴ Faculty of Economics, Nguyen Huu Canh College of Economics and Technology, Ho Chi Minh 700000, Vietnam
- ⁵ Anh Minh Global One Member Co., Ltd. for Renewable Energy (AMG), Ho Chi Minh 700000, Vietnam

Corresponding Author Email: ngodangluu@anhminhglobal.com

Copyright: ©2025 The authors. This article is published by IIETA and is licensed under the CC BY 4.0 license (http://creativecommons.org/licenses/by/4.0/).

https://doi.org/10.18280/ijsdp.200926

Received: 15 August 2025 Revised: 22 September 2025 Accepted: 27 September 2025

Available online: 30 September 2025

Keywords:

floating solar project, floating photovoltaic (FPV), economic–technical management, environmental impact

ABSTRACT

Floating solar photovoltaic (FPV) technology has emerged as an effective solution with multiple added benefits. A comparison of Meteonorm and SolarGIS datasets highlights clear seasonal variations, with annual global horizontal irradiation (GHI) exceeding 1600 kWh/m² and diffuse horizontal irradiation (DHI) accounting for around 40–50% of total solar radiation. An environmental assessment was carried out across the construction, operation and integration phases, covering air, water, soil quality and electromagnetic fields. Results indicate that all measured parameters were within the limits prescribed by Vietnamese environmental standards (QCVN), although short-term impacts such as dust, noise and localised changes in dissolved oxygen were observed. FPV also reduced water evaporation by approximately 0.023 m³/s, equivalent to an additional 96 MWh/year of hydropower generation when integrated with reservoirs. Overall, the findings confirm that FPV delivers dual economic and ecological benefits, simultaneously. To the best of our knowledge, this is the first empirical FPV study in Vietnam integrating technical, economic and environmental assessments, providing evidence to support sustainable deployment in tropical water-rich regions.

1. INTRODUCTION

Global climate change and the depletion of fossil fuel resources have created an urgent need for sustainable alternative energy sources [1]. The total amount of solar energy reaching the Earth in just one hour is nearly twice the annual energy consumption of humankind [2], highlighting its immense potential. Solar energy has therefore emerged as one of the most promising renewable solutions, with global capacity surpassing 1,000 TWh in 2021 and projected to grow by at least 25% annually in order to achieve the carbonneutrality target by 2030 [3].

In Viet Nam, the country faces the dual challenge of ensuring energy security while coping with land scarcity. Floating photovoltaic (FPV) technology is increasingly regarded as a strategic pathway. In particular, integrating FPV with hydropower enables effective utilisation of base-load characteristics and synchronised grid operation. This approach aligns with the orientations of the revised National Power Development Plan VIII and the commitment to carbon neutrality by 2050.

FPV can overcome the shortcomings of ground-mounted solar systems. It offers significant advantages such as land savings, higher efficiency compared with land-based PV [4, 5], and the ability to be deployed on a wide range of water bodies.

Since the first commercial installation in 2008, FPV deployment has expanded rapidly, with more than 600 plants established across 28 countries, predominantly in Asia [6].

Although FPV presents a major opportunity for renewable energy development, knowledge of its environmental impacts on freshwater ecosystems remains limited and urgently requires investigation [4]. This knowledge gap constrains comprehensive assessments of the technology's sustainability and hinders the formulation of effective management policies.

This study provides a case analysis of an FPV project in Central Viet Nam, a region with solar irradiation levels of 4.2–5.5 kWh/m²/day and 2,000–2,600 sunshine hours per year. The research offers a holistic assessment of FPV technology, covering economic, technical and environmental aspects throughout the three phases of preparation, construction and operation. It further examines potential challenges and impacts on freshwater ecosystems. By synthesising existing evidence and field data in Viet Nam, we identify critical knowledge gaps and propose research directions to support the sustainable development of FPV in tropical, water-rich regions. This study provides an empirical, multi-campaign EIA dataset for FPV in Vietnam and systematically compares it with two public cases (V–FPV–A/B) on reservoir conditions, design, performance, environment, and regulatory compliance.

2. OVERVIEW OF FLOATING PHOTOVOLTAICS (FPV)

2.1 Concept

FPV is an advanced solar technology defined by the deployment of PV modules directly on water surfaces. A typical FPV system consists of PV panels mounted on floating structures, anchored with mooring systems, and connected to the power grid through cables and inverters. These components are specifically designed to withstand harsh aquatic conditions such as waves, wind, fluctuating water levels and corrosion risks [7]. The choice of float material (e.g., recycled HDPE or composites) and the mooring configuration (gravity anchors, bottom-anchored, or pile-driven) determines system stability and the degree of ecological impact. Depending on the project scale, inverters may be centralised or string-based, installed either onshore or on floating platforms, with consideration of cost, maintenance, and reliability in humid environments.

2.2 Potential of floating photovoltaics

FPV is emerging as a strategic alternative to land-based PV, particularly in areas with limited agricultural land or high population density [8, 9]. By making use of underutilised water surfaces, FPV not only reduces pressure on land resources but also contributes to decarbonisation and minimises conflicts with economic sectors such as agriculture and urban development. Moreover, the natural cooling effect of water enhances module performance, mitigating the efficiency losses often observed in ground-mounted PV under high temperatures [10, 11].

Within the global energy transition, FPV plays a pivotal role in achieving net-zero emissions. The *World Energy Outlook* forecasts that the share of electricity from renewables will increase from 28.4% in 2020 to 83.6% in 2050, with solar power contributing more than 17,400 TWh-over twenty times the 2020 level [12]. To reach this target, global PV capacity must expand beyond 10,000 GW by 2050, and FPV is regarded as a key technology for addressing spatial and efficiency challenges.

A particularly promising application of FPV is its integration with existing hydropower. Installing FPV on reservoirs takes advantage of existing transmission and grid infrastructure, substantially reducing investment costs and implementation time [11, 13, 14]. This integration creates an energy synergy: FPV supplies peak electricity during the day, while hydropower can flexibly compensate for variability, thereby improving grid stability and dispatchability.

3. RESEARCH METHODOLOGY

3.1 Phases of FPV project implementation relevant to environmental impacts

3.1.1 Preparation phase

The objective of the preparation phase is to assess the feasibility of FPV deployment in Viet Nam, with a focus on increasing renewable energy production and adapting to climate change. Key activities include site surveys, preliminary technical design, preparation of project

documentation, and procedures related to compensation, support and resettlement. Overall, this phase generates minimal environmental impacts, and the associated environmental management costs are therefore negligible.

3.1.2 Construction phase

The construction phase involves the mobilisation of labour and machinery, site clearance, establishment of camps and storage areas, transportation of materials, installation of transmission lines and foundations, as well as other auxiliary works. This stage produces the most significant environmental impacts: dust and emissions from earthworks and transportation; domestic and construction wastewater; noise from mechanical equipment; and both solid and hazardous waste (such as oil, lubricants and chemicals). These impacts increase environmental management costs and require mitigation measures to be implemented from the outset of construction.

3.1.3 Operation phase

During operation, the FPV project continues to generate distinct environmental impacts. Covering the water surface may alter the thermal balance, changing temperature and evaporation rates, thereby affecting aquatic ecosystems. Dust accumulation on PV modules and mooring materials may influence reservoir water quality. In addition, electromagnetic fields generated during grid connection should be considered as a potential risk factor for both the environment and public health.

3.2 Environmental impacts of floating solar projects

3.2.1 Impacts on air quality

During the construction phase, local air quality within the project area is significantly affected by excavation and material transport activities. The main sources of emissions include:

Dust generated during the transportation of soil and rock for site levelling at the substation.

Exhaust gases and dust arising from excavation works for pole foundations and transmission lines.

Dust and emissions produced during the transport, loading and unloading of construction materials (cement, sand, stone, steel) and equipment.

The volume of dust emissions can be estimated using pollutant emission factor equations.

$$E = k \times 0.0016 \times \frac{\left(\frac{U}{2.2}\right)^{1.3}}{\left(\frac{M}{2}\right)^{1.4}} \tag{1}$$

where,

E: emission factor (kg/tonne),

k: particle size multiplier (average value 0.35),

U: average wind speed (1.6 m/s),

M: average material moisture content (18.6%).

To predict the dispersion of dust emissions from excavation activities, this study applies the Gaussian plume dispersion model. This model enables the estimation of dust concentrations at receptor points according to the following equation:

$$C_{(x,y,z)} = \frac{E}{2\pi\sigma_y\sigma_z U} \exp\left(-\frac{y^2}{2\sigma_y^2}\right)$$

$$\left[\exp\left(-\frac{(z-H)^2}{2\sigma_z^2}\right) + \exp\left(-\frac{(z+H)^2}{2\sigma_z^2}\right)\right]$$
(2)

where,

 $C_{(x,y,z)}$: dust concentration at the receptor point (mg·m⁻³),

H: effective emission source height (m),

 σ_y , σ_z : horizontal and vertical dispersion coefficients (m), which depend on transport distance and atmospheric conditions.

The application of this formula enables the quantification of dust dispersion ranges, thereby allowing comparison with current environmental standards to evaluate the level of impact.

$$C_{x} = \frac{E}{\pi \sigma_{y} \sigma_{z} \bar{u}} \exp\left[-\left(\frac{H^{2}}{2\sigma_{z}^{2}}\right)\right]$$
 (3)

where.

C: concentration of air pollutants ($mg \cdot m^{-3}$),

E: emission rate (mg·s⁻¹),

H: receptor height (m), with H = 1 m,

 σ_z : vertical atmospheric dispersion coefficient (m), expressed as a function of downwind distance x: $\sigma_z = c \cdot x^d + f$,

 σ_y : horizontal atmospheric dispersion coefficient (m), expressed as: $\sigma_y = a \cdot x^{0.894}$,

 \bar{u} : average wind speed (m·s⁻¹), here $\bar{u} = 1.6 \text{ m·s}^{-1}$.

When transporting construction materials between storage yards and the construction site, noise generated by vehicles may affect roadside residents and road users. Construction equipment for the substation, such as concrete mixers, compactors, excavators and pile drivers, can also create noise affecting the surrounding environment.

The prediction of source noise levels and the calculation of noise levels at receptor points can be estimated using the following equation:

$$L_{\Sigma} = 10 \lg \sum_{i=1}^{n} 10^{0.1.L_{i}}$$
 (4)

where,

a: the coefficient representing the influence of ground surface characteristics on the absorption and reflection of noise, with values as follows:

a = -0.1 for asphalt and concrete surfaces,

a = 0 for open bare ground without vegetation,

a = 0.1 for grass-covered soil.

3.2.2 Impacts on water quality

Surface water quality is directly influenced by the presence of FPV systems. Key parameters to be monitored include pH, total suspended solids (TSS), total dissolved solids (TDS), nutrients (N, P), and chlorophyll-a (chl-a). The shading effect of FPV reduces the amount of light penetrating the water column, thereby limiting photosynthesis and oxygen exchange. If the coverage area is too large, this may lead to an overall decline in water quality.

Solar radiation reaching the reservoir is estimated based on the average monthly sunshine hours at the installation site. As light availability decreases, the photosynthetic activity of algae and aquatic organisms is reduced, leading to fluctuations in dissolved oxygen (DO) concentrations [2, 15, 16]. Moreover, shading also affects the thermal balance: water temperature increases with solar radiation and through convective transfer from the atmosphere [17].

TDS reflects the total concentration of dissolved ions, including nutrients and essential minerals [11]. Thermal stratification in reservoirs can result in the deposition of phosphorus from the surface to the bottom layers, which may reappear during seasonal mixing events [18]. Chlorophyll-a concentration is a key biological indicator for assessing algal biomass and eutrophication levels. When FPV coverage restricts light penetration, algal biomass declines, subsequently impacting the entire aquatic food chain [19].

In addition to indirect ecological impacts, anthropogenic discharges during both construction and operation are also of concern:

Domestic wastewater from workers contains suspended solids (SS), BOD/COD, nitrogen-phosphorus compounds, and microorganisms.

Construction wastewater, generated from concrete mixing and curing as well as equipment washing, contains high levels of suspended solids, oils, and chemicals.

Stormwater runoff may carry soil, rocks and construction materials, causing turbidity and sedimentation if no adequate drainage measures are implemented.

Overall, FPV installations may induce significant alterations in the biochemical dynamics of reservoirs. The magnitude of impacts depends on the coverage area, mooring system design, and wastewater management practices during both construction and operational phases.

The maximum runoff flow rate can be estimated using the following equation:

$$Q = 0.278 KIAQ = 0.278 KIA$$

where,

Q: the flow rate (m³/s),

I: rainfall intensity (mm/h),

A: the catchment area (km²), and

K: the runoff coefficient.

3.2.3 Impacts on the soil environment

During the construction phase, the activities of workers and machinery generate various types of solid waste. Domestic waste mainly consists of paper, packaging, biodegradable organic matter, glass, plastics and metals. Without proper collection and management systems, these materials may cause localised soil pollution through biodegradation or leakage of chemical additives.

In addition, construction waste such as scrap steel and surplus materials should be recovered or recycled to minimise long-term accumulation in the environment.

Of particular concern are hazardous wastes arising from the maintenance of machinery and construction vehicles, including waste oils, solvents and cleaning chemicals. These substances have the potential to infiltrate soil, leading to long-term contamination and negatively affecting groundwater quality. Therefore, hazardous waste management requires specialised treatment processes in line with environmental regulations, in order to mitigate risks to soil ecosystems and public health.

4. CASE STUDY IN CENTRAL VIET NAM

According to the National Power Development Plan 36 [20], Viet Nam aims to increase the share of renewable energy to 15–20% by 2030 and 20–30% by 2045. Within this context, the South Central Coastal region has emerged as a strategic hub, benefitting from favourable natural conditions with up to 300 sunshine days per year and an average of 2,000–2,600 sunshine hours annually. Solar irradiation ranges from 4.19 kWh·m⁻²·day in the north to 5.5 kWh·m⁻²·day in the south, offering substantial potential for solar power development.

In addition, the Central Highlands, Southern Viet Nam and South Central regions record average solar yields of 1,387–1,534 kWh/kWp per year, comparable to global high-potential renewable energy zones. These conditions not only support the expansion of solar power but also encourage investment in other renewable sources such as wind and biomass energy.

In this study, an FPV project was deployed in the South Central region to maximise the natural advantages of high solar irradiation and available water surface area. This site provides a representative case for evaluating both the technical performance and environmental impacts of FPV under Vietnamese conditions. Meteorological and energy datasets were collected and analysed, including solar irradiation, sunshine hours and seasonal variations, in order to provide a quantitative basis for electricity generation modelling and assessment of FPV potential in the region.

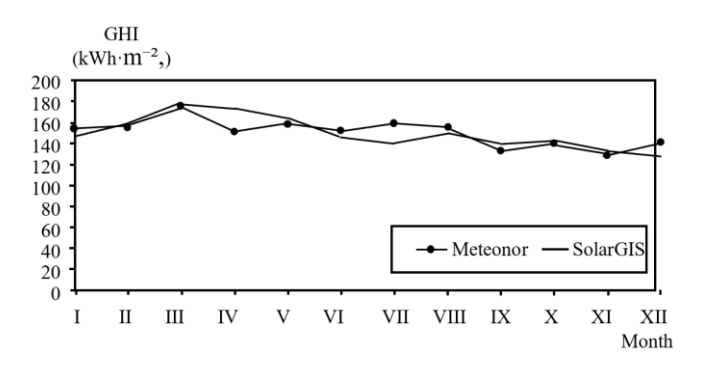


Figure 1. Monthly and annual global horizontal irradiation (GHI)

The results in Figure 1 illustrate the monthly average global horizontal irradiation (GHI, kWh·m⁻²) in the South Central region of Viet Nam, comparing data from Meteonorm and SolarGIS.

Both datasets reveal a clear seasonal variation. GHI reaches

its maximum in March, at approximately 180 kWh·m⁻², reflecting the strong sunshine characteristic of the late dry season. Thereafter, GHI gradually declines during the rainy months (June to October), fluctuating between 140 and 160 kWh·m⁻². The lowest values occur between September and November, at around 130–140 kWh·m⁻², before rising again in December.

The differences between the two datasets, Meteonorm and SolarGIS, are generally minor (< 10%); however, in certain months (e.g., April and July) the discrepancies are more pronounced, suggesting that calibration using local meteorological conditions is necessary to improve the accuracy of energy simulations.

These results indicate that the South Central region of Viet Nam benefits from stable and high levels of solar irradiation throughout the year, with an annual GHI exceeding 1,600 kWh·m⁻²·year, comparable to leading solar potential areas in Asia. This provides a favourable foundation for the deployment of FPV systems, particularly when integrated with hydropower to take advantage of existing infrastructure and optimise power output.

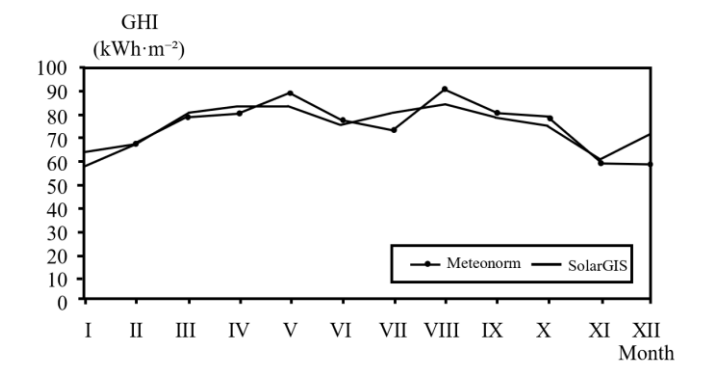


Figure 2. Monthly and annual average diffuse horizontal irradiation (DHI)

Figure 2 presents the monthly average diffuse horizontal irradiation (DHI, kWh·m $^{-2}$) in the South Central region, based on Meteonorm and SolarGIS data. The results show clear seasonal variations in DHI, reflecting changes in atmospheric conditions and cloud cover. Between March and May, DHI rises sharply, peaking in August at around 90–95 kWh·m $^{-2}$. This coincides with the rainy season, when the share of diffuse radiation increases due to the scattering of sunlight by clouds and moisture.

Table 1. Monthly and annual average diffuse horizontal irradiation	(DE	H)	į
---	-----	----	---

Month / Data Source	Meteonorm	SolarGIS	Deviation Assessment ΔDHI *100/DHI _{Meteonorm} (%)
I	58	64	11.0
II	67	66	1.3
III	78	80	2.9
IV	79	82	4.3
V	88	81	7.5
VI	76	74	2.2
VII	72	80	11.0
VIII	89	83	6.6
IX	79	77	2.1
X	77	74	3.3
XI	58	60	3.5
XII	57	70	23.4
Year	878	894	1.8

Conversely, the data in Table 1 show that during the dry season (January–February and November–December), DHI values are lowest, around 60–65 kWh·m⁻², indicating that direct sunlight predominates. A comparison of the two datasets shows a high level of consistency, with only small differences (< 5%). This confirms the reliability of the data for solar potential modelling. Nonetheless, localised differences during transitional months (June and September) highlight the need for field measurements to reduce forecasting errors.

From a practical perspective, high DHI levels in the rainy season may reduce PV module efficiency due to the predominance of diffuse light. However, in FPV systems, the cooling effect of the water surface can partially offset this efficiency loss. Therefore, a combined analysis of GHI and DHI provides an essential basis for accurately assessing potential and optimising FPV design in the South Central region of Viet Nam.

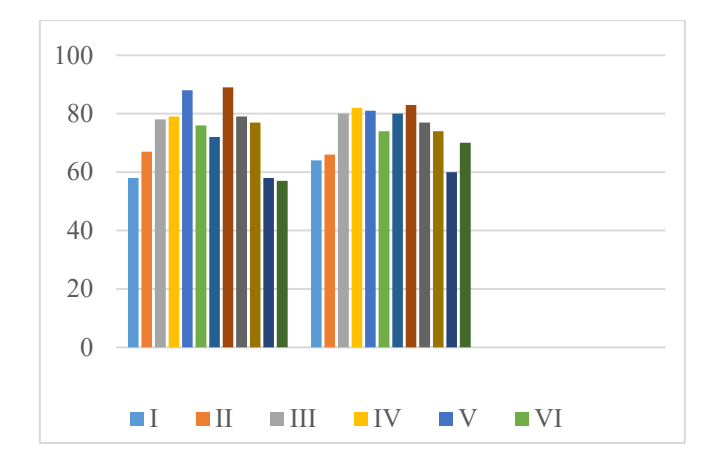


Figure 3. Monthly average diffuse irradiance (DHI)

Overall, both data sources exhibit a similar variation trend,

with DHI values ranging from 57–89 kWh·m⁻²·month. The highest DHI is recorded in August (89 kWh·m⁻² according to Meteonorm; 83 kWh·m⁻² according to SolarGIS), reflecting the strong scattering intensity during the rainy season. In contrast, January, November, and December show the lowest values (57–64 kWh·m⁻²), consistent with dry season conditions when direct radiation predominates.

The discrepancy between the two datasets is generally minor, with an annual mean error of only 1.8%. However, when compared to Figure 3, some months have significant deviations, such as January (11.0%) and December (23.4%), suggesting that the satellite-based dataset (SolarGIS) captures cloud cover, humidity, and atmospheric conditions differently from the interpolated meteorological dataset (Meteonorm). This highlights the need for on-site measurements to calibrate and reduce model errors in PV system design.

In total, annual DHI values range from 878 kWh·m⁻² (Meteonorm) to 894 kWh·m⁻² (SolarGIS), indicating high reliability when using either dataset to estimate solar energy potential in the study area. Notably, DHI accounts for approximately 40–50% of total global horizontal irradiance (GHI), reflecting the characteristic atmospheric conditions of Central Vietnam with its prolonged rainy season and high cloud frequency.

This has important implications for FPV system design, as module performance may be affected when diffuse irradiance dominates. At the same time, the cooling effect of the water surface helps maintain a more stable energy conversion efficiency compared to land-based PV.

4.1 Air quality measurement results of the project

The results in Table 2 indicate that ambient air quality monitoring at the three surveyed locations (AQ1, AQ2, AQ3) was compared against the permissible thresholds defined in QCVN 05:2013/BTNMT and QCVN 26:2010/BTNMT.

Table 2. Air environment quality analysis results

No.	Parameter	Unit	Test Method		Result		QCVN 05:2013/B TNMT (1- Hour Average)	QCVN 05:2013/BTN MT (8-Hour Average)	QCVN 05:2013/BTN MT (24-Hour Average)	QCVN 05:2013/BTN MT (Annual Average)	QCVN 26:201 0/ BTNM T
				AQ 1	A Q2	AQ 3					
1	Noise	dBA	TCVN 7878- 2:2010	50.5	56. 3	51.7	-	-	-	-	70**
2	Total Suspended Particles (TSP)	mg⋅ m ⁻³	TCVN 5067:19 95	0.02	0.0 8	0.04	0.3	-	0.2		-
3	Sulphur Dioxide (SO ₂)	mg· m ⁻³	TCVN 5971:19 95	0.02	0.0 1	0.03	0.35	-	0.05		-
4	Nitrogen Oxides NOx	mg· m ⁻³	HD77- PPDN- NOx	0.05	0.0	0.03	0.2	-	0.04		-
5	Carcbon Monoxide (CO)	m_{-3}	HD24- LM-CO	KP H	KP H	KP H	30	10	-		-
6	Lead (Pb)	mg· m³	TCVN 5067:19 95	KP H	KP H	KP H	-	-	0.5		-

Noise levels ranged from 50.5–56.3 dBA, well below the limit of 70 dBA (QCVN 26:2010/BTNMT). This suggests that the acoustic environment in the area remains within acceptable limits and does not pose risks to public health.

Total Suspended Particles (TSP) were measured at $0.02-0.08~\text{mg}\cdot\text{m}^{-3}$, lower than the regulatory thresholds for 1-hour $(0.3~\text{mg}\cdot\text{m}^{-3})$ and 24-hour averages $(0.2~\text{mg}\cdot\text{m}^{-3})$. These results indicate that construction and traffic activities in the area have not generated dust pollution levels exceeding the standards.

 SO_2 concentrations ranged from $0.01-0.03~mg\cdot m^{-3}$, significantly below the limits of $0.35~mg\cdot m^{-3}$ (1-hour average) and $0.05~mg\cdot m^{-3}$ (24-hour average). NO_x levels were recorded at $0.03-0.05~mg\cdot m^{-3}$, also under the thresholds of $0.2~mg\cdot m^{-3}$ (1-hour) and $0.04~mg\cdot m^{-3}$ (24-hour). However, the value at AQ1 reached $0.05~mg\cdot m^{-3}$, approaching the 24-hour limit, suggesting that this site may be locally affected by construction vehicles or traffic activities.

Both CO and Pb were not detected (N.D.), indicating no significant emission sources from fossil fuel combustion or industrial activity in the study area.

Overall, the findings demonstrate that the air quality within the project area meets the current QCVN requirements, with most parameters remaining well below the permissible thresholds. Nonetheless, the localised NO_x concentration at AQ1 should be continuously monitored during the construction phase to prevent exceedances when traffic and machinery intensity increases.

From a practical perspective, these results provide scientific evidence that the air quality impact of the FPV project during the initial survey phase is negligible. However, dust and exhaust control measures should still be implemented during construction to ensure that air quality is maintained at a safe level.

4.2 Results on water quality impacts

Table 3 presents the analysis results for 16 surface water quality parameters at three sampling locations (MN1, MN2, MN3), compared with the standards of QCVN 08-MT:2015/BTNMT.

NT.	D	WT .*4	To a Made a		Result		QCVN 08-
No.	Parameter	Unit	Test Method -	MN1	MN2	MN3	MT:2015/BTNMT
1	рН	-	TCVN 6492:2011	7.2	7.1	7.1	5.5-9
2	DO	mg/l	TCVN 7325:2004	5.2	5.6	5.1	4
3	TSS	mg/l	TCVN 6625:2000	12.4	14.2	18.5	50
4	COD	mg/l	SMEWW 5220C:2012	14.3	11.9	17.2	30
5	BOD5	mg/l	TCVN 6001-1:2008	6.7	7.2	11.4	15
6	Coliform	MNP/100ml	TCVN 6187-2:2009	740	670	680	7500
7	Nitrate	mg/l	SMEWW 4500-NO3- E:2012	1.6	1.8	1.9	10
8	Nitrite	mg/l	TCVN 6187:1996	KPH	KPH	KPH	0.05
9	Ammonium	mg/l	EPA Metthod 350.2	KPH	KPH	KPH	0.9
10	Copper	mg/l	SMEWW 3111.B:2012	< 0.03	< 0.03	< 0.03	0.5
11	Iron	mg/l	SMEWW 3111.B:2012	< 0.08	< 0.08	< 0.08	0.4
12	Nickel	mg/l	SMEWW 3111.B:2012	KPH	KPH	KPH	0.1
13	Zinc	mg/l	SMEWW 2012-3500-Zn.B	0.08	0.06	0.09	1.5
14	Lead	mg/l	SMEWW 3111B:2012	KPH	KPH	KPH	0.05
15	Total Chromium	mg/l	SMEWW 3500-Cr.B:2012	КРН	КРН	КРН	0.5
16	Phosphate	mg/l	TCVN 6202:2008	KPH	KPH	KPH	0.3

The findings indicate that all parameters remain within the permissible limits, reflecting relatively good water quality in the project reservoir area with no clear evidence of pollution impacts.

pH values ranged between 7.1 and 7.2, within the neutral range, suitable for aquatic life (permissible range: 5.5-9).

Dissolved Oxygen (DO) levels reached 5.1-5.6 mg/L, higher than the minimum threshold of 4 mg/L, indicating oxygen-rich water conditions favourable for aquatic ecosystems.

Total Suspended Solids (TSS) were recorded at 12.4–18.5 mg/L, much lower than the limit of 50 mg/L, showing that the water is relatively clear and less affected by sedimentation or construction activities.

COD (11.9-17.2 mg/L) and BOD₅ (6.7-11.4 mg/L) were both below their respective limits (30 mg/L and 15 mg/L), reflecting moderate to low levels of organic pollution.

Coliform counts ranged between 670-740 MPN/100ml, far below the threshold of 7500, suggesting no significant microbial contamination from domestic wastewater sources.

Nutrient compounds (nitrate 1.6-1.9 mg/L; nitrite and ammonium not detected) were all at low levels, posing no risk of eutrophication.

Heavy metals (Cu < 0.03 mg/L; Fe < 0.08 mg/L; Zn 0.06-0.09 mg/L; Pb, Ni, and Cr not detected) were many times lower than the regulatory standards, confirming the absence of industrial pollution in the surveyed area.

Phosphate was not detected, further supporting the conclusion that the risk of reservoir eutrophication is low.

In summary, the results show that surface water in the FPV project area meets good quality standards according to QCVN, with low concentrations of suspended solids, organic matter, and microorganisms. This provides favourable conditions for the deployment of a floating solar power system without exerting significant pressure on the existing freshwater ecosystem. However, during both construction and operation phases, strict management of domestic wastewater and construction materials is required to avoid increases in TSS or organic pollution, especially during the rainy season when surface runoff is more likely.

Table 4. Result of electric field intensity

				Result	QCVN 03-	
No.	Parameter	Unit	Method	ÐT	MT:2015/B TNMT	
1	Industrial frequency electric field intensity	kV/ m	Rapid meter HI3604	1.164	. 5	
2	High- frequency electric field intensity	kV/ m	Rapid meter HI3604	0.877	≤ 5	

The results in Table 4 on electric field intensity monitoring at the FPV project site include both industrial frequency and high-frequency measurements.

The industrial frequency electric field intensity was recorded at 1.164 kV/m, significantly lower than the permissible threshold of 5 kV/m set out in QCVN 03-MT:2015/BTNMT.

The high-frequency electric field intensity was measured at $0.877~\mathrm{kV/m}$, also within the safety limits for both the environment and public health.

ELF/LF (50–3 000 Hz), IF (3 kHz–100 kHz), RF (0.1–6 GHz). Spectral plots and maximum values at 0.3 m / 1 m / accessible areas are provided for critical points (inverter, DC/AC cable routes, floating walkways, control area). Compliance follows IEC 62226 (≤ 100 kHz) and ICNIRP 2020 (≥ 100 kHz). Long-term exposure is reported using TWA and P95 values, including BESS scenarios (2–20 kHz, shielding, setback distances).

These findings demonstrate that the FPV project does not generate electric field emissions exceeding regulatory standards and fully complies with Vietnam's requirements on electromagnetic radiation safety. The measured values represent only around 20–25% of the permissible limits, indicating a wide safety margin and low risk for both operational staff and nearby communities.

In practical terms, this result highlights that FPV systems can be integrated into the existing power grid without adding pressure in terms of electromagnetic emissions. Nevertheless, regular monitoring remains necessary to ensure long-term safety, particularly when expanding capacity or integrating with energy storage systems (BESS) and smart grids in the future.

The annual supplementary hydropower generation (Ehyd), derived from the volume of water saved by installing the floating solar PV (FPV) system, can be estimated using the following expression:

$$E_{hyd} = \frac{\rho g H \eta \Delta V_{year}}{3.6 \times 10^6} \text{ (MWh)}$$
 (5)

where

 ΔV_{year} : Annual water savings (m³·y⁻¹) Volume of water conserved from evaporation due to PV coverage

H: Effective head (m)

 η : Turbine–generator efficiency (–)

 3.6×10^6 : Conversion factor from joules (J) to kilowatthours (kWh)

This formula shows that the volume of water conserved through reduced evaporation ($\Delta Vyear$) is converted into

hydraulic potential energy, which is then transformed into additional electricity generation, depending on the available head and the efficiency of the equipment.

Table 5. Additional power generation

Parameter	Unit	Value	Cignificance
rarameter	Unit	varue	Significance
			Designed energy
Turbine capacity	MWh	87.5	capacity of the
			turbine
			Water flow
Operating flowm	m^3/s	68.5	through the
			turbine
Reduced			Volume of water
1100000	m^3/s	0.0231	conserved from
evaporation after PV installation	m ³ /S	0.0231	evaporation due
P v Installation			to PV coverage
Ei14			Additional
Equivalent			electricity
electricity from	kWh	29.567	generated from
reduced			conserved water
evaporation			(per unit)
Additional daily			Extra electricity
electricity	kWh	709.65	the plant can
generation			produce each day
Additional annual			Total extra
electricity	1-3371-	06 495 05	electricity
generation (above	kWh	96,485.95	generated
design)			annually

Table 5 presents the key operating parameters of the hydropower unit when integrated with a floating solar PV (FPV) system.

Full meteorological boundary conditions including air temperature (30–32°C), RH (55–65%), wind speed at 10 m (4–6 m s⁻¹; converted to $u_2 \approx 3-5$ m s⁻¹ via FAO-56), daily shortwave radiation (6.3–6.7 kWh m⁻² day⁻¹), and net radiation calculated using FAO-56. Site area is ~50 ha, with FPV wind shielding coefficient assumed 0.6–0.8. Meteorological data are from long-term provincial records (Phan Thiết, Bình Thuận) and project design data (EVN/DHD). Uncertainty bounds are included.

The turbine unit is designed with a capacity of 87.5 MWh, corresponding to its rated generation output.

The operating flow reaches 68.5 m³/s, representing the average water volume passing through the turbine under normal operating conditions.

Table 6 analyzes the standardized LCOE, full assumptions:

- Transparent CAPEX breakdown (modules, floaters, mooring/anchoring, DC/AC cabling, on-shore infra, SCADA, soft cost, contingency).
- OPEX items (O&M, environmental monitoring, insurance, water lease).
- Financial parameters (discount rate/WACC, inflation handling, currency base year).
- Lifetime, PR, degradation, availability, curtailment assumptions.

We also added sensitivity analyses: (i) tornado (single variable), (ii) 2D PR×CAPEX surface, (iii) Monte Carlo (10,000 samples, 95% CI).

Table 6 illustrates the sensitivity and scenarios (including cases where mooring costs are higher); all inputs are traceable back to the quotations/BoQ or published benchmarks. With the documented assumptions, the FPV option still yields a lower LCOE, while the sensitivity analysis clearly indicates the conditions under which this ranking may change.

Table 6. LCOE assumptions (Compact but complete)

Category	Parameter	Unit	Base	Sensitivity / Source
	Installed capacity	MWp	47.5	— Da Mi site
Technical	Performance Ratio (PR)	-	0.80	± 5% SCADA benchmark
recimicai	Degradation	%/year	0.6	± 50% Datasheet
	Lifetime	years	25	— Standard
	PV modules & structure	USD/kWp	450	± 10% Vendor quotation
	Floaters + anchoring + mooring	USD/kWp	320	± 15% Site-specific
CAPEX	DC/AC cables & interconnection	USD/kWp	80	\pm 10% Engineering
	SCADA & soft cost	USD/kWp	50	± 10% Benchmark
	Contingency	USD/kWp	50	\pm 15% 10% subtotal
	O&M	USD/kWp·yr	15	± 20% Service + labor
OPEX	Environmental monitoring	USD/kWp·yr	5	± 20% Annualized
	Insurance & lease	USD/kWp·yr	5	± 20% Policy
	Discount rate (WACC)	%	7	± 2% Finance base
Financial	Inflation	%	2.5	± 1% CPI Vietnam
	Curtailment	% energy	2	± 50% Grid dispatch
Othor	Exchange rate base year	-	2025 USD	— Fixed
Other	Reference standard	-	IEC/DNV	— VN + Intl benchmarks

One of the notable benefits of FPV is the reduction of water evaporation on the reservoir surface due to the shading effect of solar panels. Calculations show that evaporation is reduced by 0.0231 m³/s. When converted into electricity, this conserved water corresponds to 29.567 kWh per unit, by increasing the effective flow available to the turbine.

This translates into an additional ~709.65 kWh per day, equivalent to 96,485.95 kWh annually, compared to the original design. Such figures not only enhance the efficiency of water resource utilisation but also increase the overall electricity output of the FPV-hydropower hybrid system.

From a practical perspective, the evaporation reduction effect highlights the dual benefit of FPV: conserving water resources while boosting electricity generation without significant additional operating costs. This is a critical factor in assessing the sustainability and long-term advantages of FPV in tropical monsoon climates, where high evaporation rates can otherwise affect hydropower efficiency.

5. DISCUSSION OF RESEARCH RESULTS

We compare the case studies with V–FPV–A (FPV 47.5 MWp, 2019) and V–FPV–B (Northern hydropower reservoir context). The research findings indicate that floating solar photovoltaic (FPV) systems in the South Central region of Vietnam not only take advantage of abundant solar irradiation but also provide multiple co-benefits in terms of environmental protection and energy efficiency. Compared with ground-mounted PV, FPV reduces land occupation, mitigates land-use conflicts with agriculture and urban development, and benefits from the cooling effect of water surfaces, thereby improving photovoltaic conversion efficiency. Similar findings have been reported in previous studies [2-24].

Environmental analyses show that both air and water quality in the project area remain within permissible thresholds defined by QCVN standards, demonstrating that the direct environmental impacts during construction and operation are limited. However, monitoring results also revealed potential risks, such as localised dust increases during construction and variations in dissolved oxygen (DO) due to surface coverage. This is consistent with the observations of previous studies [14, 21, 25, 26], which emphasise that FPV may affect algal photosynthesis and aquatic dynamics if the coverage area exceeds safe thresholds.

A particularly important finding is the evaporation reduction effect from surface coverage, which not only helps to maintain stable water resources for hydropower generation but also provides an additional ~96 MWh of electricity annually. This clearly illustrates the synergistic benefits of FPV–hydropower integration, a "win–win" mechanism that conserves water resources while enhancing the economic performance of hydropower plants. These results reinforce the conclusions of previous studies regarding the dual ecological–energy value of FPV [19, 27-29].

From an economic perspective, the levelised cost of electricity (LCOE) for FPV is estimated to be lower than that of ground-mounted PV, owing to the use of existing transmission infrastructure and the avoidance of land acquisition costs. This aligns with global trends where FPV is recognised as a strategic technology to expand PV capacity in contexts of land scarcity [6, 12].

Nevertheless, several challenges were identified. First, the lack of long-term measurement data in Vietnam may distort electricity yield forecasts, especially during transitional months when cloud cover fluctuates significantly. Second, the management of construction waste and hazardous materials requires close attention to prevent soil and water contamination. Third, the long-term impacts of electromagnetic fields and changes in aquatic ecosystems remain to be continuously monitored.

In summary, this study provides the first empirical evidence in the South Central region of Vietnam on the environmental impacts and techno-economic benefits of FPV. Furthermore, it is the first study worldwide to assess techno-economic performance based on real-world environmental impact monitoring in a geographically favourable area for scaling up floating solar deployment. These findings fill a critical research gap on FPV in Vietnam and provide important policy implications for integrating FPV into the national Power Development Plan VIII, thereby contributing to the net-zero emissions target by 2050.

REFERENCES

- [1] Armstrong, A., Page, T., Thackeray, S.J., Hernandez, R.R., Jones, I.D. (2020). Integrating environmental understanding into freshwater floatovoltaic deployment using an effects hierarchy and decision trees. Environmental Research Letters, 15(11): 114055. https://doi.org/10.1088/1748-9326/abbf7b
- [2] Cagle, A.E., Armstrong, A., Exley, G., Grodsky, S.M., Macknick, J., Sherwin, J., Hernandez, R.R. (2020). The land sparing, water surface use efficiency, and water surface transformation of floating photovoltaic solar energy installations. Sustainability, 12(19): 8154. https://doi.org/10.3390/su12198154
- [3] Château, P.A., Wunderlich, R.F., Wang, T.W., Lai, H.T., Chen, C.C., Chang, F.J. (2019). Mathematical modeling suggests high potential for the deployment of floating photovoltaic on fish ponds. Science of the Total Environment, 687: 654-666. https://doi.org/10.1016/j.scitotenv.2019.05.420
- [4] Decision 500/QD-TTg. (2023). Approval of National Power Development Plan VIII. https://en.baochinhphu.vn/decision-approving-national-power-development-plan-8-111230614195813455.htm.
- [5] de Lima, R.L.P., Paxinou, K., C. Boogaard, F., Akkerman, O., Lin, F.Y. (2021). In-situ water quality observations under a large-scale floating solar farm using sensors and underwater drones. Sustainability, 13(11): 6421. https://doi.org/10.3390/su13116421
- [6] Exley, G., Page, T., Thackeray, S.J., Folkard, A.M., Couture, R.M., Hernandez, R.R., Cagle, A.E., Salk, K.R., Clous, L., Whittaker, P., Chipps, M., Armstrong, A. (2022). Floating solar panels on reservoirs impact phytoplankton populations: A modelling experiment. Journal of Environmental Management, 324: 116410. https://doi.org/10.1016/j.jenvman.2022.116410
- [7] Gadzanku, S., Mirletz, H., Lee, N., Daw, J., Warren, A. (2021). Benefits and critical knowledge gaps in determining the role of floating photovoltaics in the energy-water-food nexus. Sustainability, 13(8): 4317. https://doi.org/10.3390/su13084317
- [8] Gibson, L., Wilman, E.N., Laurance, W.F. (2017). How green is 'green' energy? Trends in Ecology & Evolution, 32(12): 922-935. https://doi.org/10.1016/j.tree.2017.09.007
- [9] Gorjian, S., Sharon, H., Ebadi, H., Kant, K., Scavo, F.B., Tina, G.M. (2021). Recent technical advancements, economics and environmental impacts of floating photovoltaic solar energy conversion systems. Journal of Cleaner Production, 278: 124285. https://doi.org/10.1016/j.jclepro.2020.124285
- [10] Grodsky, S.M. (2021). Matching renewable energy and conservation targets for a sustainable future. One Earth, 4(7): 924-926. https://doi.org/10.1016/j.oneear.2021.07.001
- [11] Hosenuzzaman, M., Rahim, N.A., Selvaraj, J., Hasanuzzaman, M., Malek, A.B.M.A., Nahar, A. (2015). Global prospects, progress, policies, and environmental impact of solar photovoltaic power generation. Renewable and Sustainable Energy Reviews, 41: 284-297. https://doi.org/10.1016/j.rser.2014.08.046
- [12] Jäger-Waldau, A. (2022). Snapshot of photovoltaics February 2022. EPJ Photovoltaics, 13: 9. https://doi.org/10.1051/epjpv/2022010

- [13] Ji, Q., Li, K., Wang, Y., Feng, J., Li, R., Liang, R. (2022). Effect of floating photovoltaic system on water temperature of deep reservoir and assessment of its potential benefits, a case on Xiangjiaba Reservoir with hydropower station. Renewable Energy, 195: 946-956. https://doi.org/10.1016/j.renene.2022.06.096
- [14] Jing, R., Lin, Y., Khanna, N., Chen, X., Wang, M., Liu, J., Lin, J. (2021). Balancing the energy trilemma in energy system planning of coastal cities. Applied Energy, 283: 116222. https://doi.org/10.1016/j.apenergy.2020.116222
- [15] Lee, N., Grunwald, U., Rosenlieb, E., Mirletz, H., Aznar, A., Spencer, R., Cox, S. (2020). Hybrid floating solar photovoltaics-hydropower systems: Benefits and global assessment of technical potential. Renewable Energy, 162: 1415-1427. https://doi.org/10.1016/j.renene.2020.08.080
- [16] M G Rocha, S., Armstrong, A., Thackeray, S.J., Hernandez, R.R., M Folkard, A. (2024). Environmental impacts of floating solar panels on freshwater systems and their techno-ecological synergies. Environmental Research: Infrastructure and Sustainability, 4(4): 042002. https://doi.org/10.1088/2634-4505/ad8e81
- [17] Mugnier, D. (2022). Photovoltaic Power Systems Programme Annual Report 2022. IEA: Paris, France. https://iea-pvps.org/wp-content/uploads/2023/04/PVPS_Annual_Report_2022_v7-1.pdf.
- [18] Nobre, R., Rocha, S.M., Healing, S., Ji, Q., Boulêtreau, S., Armstrong, A., Cucherousset, J. (2024). A global study of freshwater coverage by floating photovoltaics. Solar Energy, 267: 112244. https://doi.org/10.1016/j.solener.2023.112244
- [19] Oliveira, P.M.B., Almeida, R.M., Cardoso, S.J. (2024). Effects of floating photovoltaics on aquatic organisms: A review. Hydrobiologia, 852(12): 3155-3170. https://doi.org/10.1007/s10750-024-05686-0
- [20] Pimentel Da Silva, G.D., Magrini, A., Branco, D.A.C. (2019). A multicriteria proposal for large-scale solar photovoltaic impact assessment. Impact Assessment and Project Appraisal, 38(1): 3-15. https://doi.org/10.1080/14615517.2019.1604938
- [21] Ray, N.E., Holgerson, M.A., Grodsky, S.M. (2024). Immediate effect of floating solar energy deployment on greenhouse gas dynamics in ponds. Environmental Science & Technology, 58(50): 22104-22113. https://doi.org/10.1021/acs.est.4c06363
- [22] Sahu, A., Yadav, N., Sudhakar, K. (2016). Floating photovoltaic power plant: A review. Renewable and Sustainable Energy Reviews, 66: 815-824. https://doi.org/10.1016/j.rser.2016.08.051
- [23] Spencer, R.S., Macknick, J., Aznar, A., Warren, A., Reese, M.O. (2018). Floating photovoltaic systems: Assessing the technical potential of photovoltaic systems on man-made water bodies in the continental United States. Environmental Science & Technology, 53(3): 1680-1689. https://doi.org/10.1021/acs.est.8b04735
- [24] Tao, M., Hamada, H., Druffel, T., Lee, J.J., Rajeshwar, K. (2020). Review—Research needs for photovoltaics in the 21st century. ECS Journal of Solid State Science and Technology, 9(12): 125010. https://doi.org/10.1149/2162-8777/abd377
- [25] Trapani, K., Redón Santafé, M. (2014). A review of floating photovoltaic installations: 2007-2013. Progress

- in Photovoltaics: Research and Applications, 23(4): 524-532. https://doi.org/10.1002/pip.2466
- [26] World Bank Group, ESMAP, SERIS. (2018). Where Sun Meets Water: Floating Solar Market Report-Executive Summary (World Bank Group). https://documents1.worldbank.org/curated/en/57994154 0407455831/pdf/Floating-Solar-Market-Report-Executive-Summary.pdf.
- [27] World Energy Outlook 2021. (2022). https://www.iea.org/reports/world-energy-outlook-2021.
- [28] Wu, D., Grodsky, S.M., Xu, W., Liu, N., Almeida, R.M.,
- Zhou, L., Miller, L.M., Roy, S.B., Xia, G., Agrawal, A.A., Houlton, B.Z., Flecker, A.S., Xu, X. (2023). Observed impacts of large wind farms on grassland carbon cycling. Science Bulletin, 68(23): 2889-2892. https://doi.org/10.1016/j.scib.2023.10.016
- [29] Yang, P., Chua, L.H.C., Irvine, K.N., Nguyen, M.T., Low, E.W. (2022). Impacts of a floating photovoltaic system on temperature and water quality in a shallow tropical reservoir. Limnology, 23(3): 441-454. https://doi.org/10.1007/s10201-022-00698-y